Journal of Biomolecular NMR, 7 (1996) 315–330
ESCOM

J-Bio NMR 352

Possible role of a short extra loop of the long-chain flavodoxin from *Azotobacter chroococcum* in electron transfer to nitrogenase: Complete ^{1}H, ^{15}N and ^{13}C backbone assignments and secondary solution structure of the flavodoxin*

Sjaak Peelen[a], Sybren S. Wijmenga[b], Paul J.A. Erbel[a], Robert L. Robson[c], Robert R. Eady[d] and Jacques Vervoort[a,**]

[a]*Department of Biochemistry, Agricultural University, Dreijenlaan 3, NL-6703 HA Wageningen, The Netherlands*
[b]*SON/NWO National HF-NMR Facility, University of Nijmegen, Toernooiveld, NL-6525 ED Nijmegen, The Netherlands*
[c]*School of Animal and Microbial Sciences, University of Reading, P.O. Box 228, Reading RG6 6AJ, U.K.*
[d]*Nitrogen Fixation Laboratory, John Innes Centre, Norwich NRA 7HH, U.K.*

Received 24 January 1996
Accepted 27 March 1996

Keywords: Triple-resonance 3D NMR; Resonance assignments; Chemical shifts; Protein secondary structure; Electron transfer; Nitrogen fixation

Summary

The ^{1}H, ^{15}N and ^{13}C backbone and ^{1}H and ^{13}C beta resonance assignments of the long-chain flavodoxin from *Azotobacter chroococcum* (the 20-kDa *nifF* product, flavodoxin-2) in its oxidized form were made at pH 6.5 and 30 °C using heteronuclear multidimensional NMR spectroscopy. Analysis of the NOE connectivities, together with amide exchange rates, $^{3}J_{H^{N}H^{\alpha}}$ coupling constants and secondary chemical shifts, provided extensive solution secondary structure information. The secondary structure consists of a five-stranded parallel β-sheet and five α-helices. One of the outer regions of the β-sheet shows no regular extended conformation, whereas the outer strand β4/6 is interrupted by a loop, which is typically observed in long-chain flavodoxins. Two of the five α-helices are nonregular at the N-terminus of the helix. Loop regions close to the FMN are identified. Negatively charged amino acid residues are found to be mainly clustered around the FMN, whereas a cluster of positively charged residues is located in one of the α-helices. Titration of the flavodoxin with the Fe protein of the *A. chroococcum* nitrogenase enzyme complex revealed that residues Asn^{11}, Ser^{68} and Asn^{72} are involved in complex formation between the flavodoxin and Fe protein. The interaction between the flavodoxin and the Fe protein is influenced by MgADP and is of electrostatic nature.

Introduction

Flavodoxins are small redox proteins that serve as low-potential electron carriers. They all contain a noncovalently bound FMN molecule, which acts as the electron-accepting/-donating group (Mayhew and Tollin, 1992). The FMN may exist in three different redox states: oxidized, one-electron-reduced (i.e. semiquinone), and two-electron-reduced (i.e. hydroquinone). In the semiquinone redox-state (SQ) the isoalloxazine part of the FMN has a paramagnetic character due to the unpaired electron on the isoalloxazine moiety (Fritz et al., 1973). Three-dimensional structures of several flavodoxins are known (Watenpaugh et al., 1973; Burnett et al., 1974; Ludwig et al., 1976; Smith et al., 1977,1983; Fukuyama et al., 1990; Van Mierlo et al., 1990a; Stockman et al., 1990; Watt et al.,

**Supplementary Material* is available on request, comprising a Materials and Methods section for the expression and purification of the *A. chroococcum* flavodoxin, a Table S1 containing the parameters of the titration of *A. chroococcum* flavodoxin with the Fe protein, and a Table S2 containing the ^{15}N, H^{N}, $^{13}C^{\alpha}$, $^{1}H^{\alpha}$, $^{13}C^{\beta}$, $^{1}H^{\beta}$ and ^{13}CO chemical shifts.

**To whom correspondence should be addressed.

Abbreviations: SQ, semiquinone; FMN, riboflavin 5'-monophosphate; nif, nitrogen fixation; TSP, 3-(trimethylsilyl)propionate sodium salt; DSS, 2,2-dimethyl-2-silapentane-5-sulfonate sodium salt.

A

```
          10                  30                  50
           |         |         |         |         |         |
CACGCAGCCAGAGGTTTAAGTTATGGCCAAGATTGGACTCTTCTTCGGTAGCAACACCGG
                     M  A  K  I  G  L  F  F  G  S  N  T  G  ( 13)
          70                  90                 110
           |         |         |         |         |         |
TAAAACCCGCAAGGTCGCCAAGTCGATCAAGAAGCGTTTCGACGACGAAACCATGTCCGA
 K  T  R  K  V  A  K  S  I  K  K  R  F  D  D  E  T  M  S  D  ( 33)
         130                 150                 170
           |         |         |         |         |         |
TGCAGTGAACGTCAACCGCGTTTCCGCGGAAGACTTCGCCCAGTACCAGTTCCTGATCCT
 A  V  N  V  N  R  V  S  A  E  D  F  A  Q  Y  Q  F  L  I  L  ( 53)
         190                 210                 230
           |         |         |         |         |         |
GGGTACCCCGACCCTTGGCGAAGGCGAACTCCCGGGCCTCTCCTCCGACTGCGAGAACGA
 G  T  P  T  L  G  E  G  E  L  P  G  L  S  S  D  C  E  N  E  ( 73)
         250                 270                 290
           |         |         |         |         |         |
GAGCTGGGAAGAGTTCCTGCCGAAAATCGAAGGCCTGGACTTCAGCGGCAAGACCGTGGC
 S  W  E  E  F  L  P  K  I  E  G  L  D  F  S  G  K  T  V  A  ( 93)
         310                 330                 350
           |         |         |         |         |         |
TCTGTTCGGTCTGGGCGACCAGGTCGGCTATCCCGAGAACTTCCTCGATGCCATGGGCGA
 L  F  G  L  G  D  Q  V  G  Y  P  E  N  F  L  D  A  M  G  E  (113)
         370                 390                 410
           |         |         |         |         |         |
ACTGCATTCCTTCTTCACCGAGCGCGGTGCCAAGGTCGTAGGCGCCTGGTCGACCGACGG
 L  H  S  F  F  T  E  R  G  A  K  V  V  G  A  W  S  T  D  G  (133)
         430                 450                 470
           |         |         |         |         |         |
CTACGAGTTCGAAGGCTCCACCGCAGTGGTTGACGGCAAGTTCGTCGGCCTGGCGCTGGA
 Y  E  F  E  G  S  T  A  V  V  D  G  K  F  V  G  L  A  L  D  (153)
         490                 510                 530
           |         |         |         |         |         |
TCTGGACAACCAGAGCGGCAAGACCGACGAGCGCGTCGCTGCCTGGCTGGCACAGATCGC
 L  D  N  Q  S  G  K  T  D  E  R  V  A  A  W  L  A  Q  I  A  (173)
         550                 570
           |         |         |
TCCCGAGTTCGGCCTGTCCCTGTAAGGGTCGATCCGGTCATGCAGCTTT
 P  E  F  G  L  S  L
```

B

```
D. vulgaris     MPKALIVYGSTTGNTEYTAETIARELADAGYEVDSRDAASVEAGGLFEGFDLVLL ( 55)
A. nidulans     MAKIGLFYGTQTGVTQTIAESIQQEFGGESIV-DLNDIANADASD-LNAYDYLII ( 53)
A. chroococcum  MAKIGLFFGSNTGKTRKVAKSIKKRFDDETMS-DAVNVNRVSAED-FAQYQFLIL ( 53)
                |         |         |         |         |         |
                1        10        20        30        40        50

D. vulgaris     GCSTWGD------DSIELQDDFIPLFDSL-EETGAQGRKVACFGCGDS-SYE-YF (101)
A. nidulans     GCPTWNVGEL--------QSDWEGIYDD-LDSVNFQGKKVAYFGAGDQVGYSDNF ( 99)
A. chroococcum  GTPTLGEGELPGLSSDCENESWEEFL-PKIEGLDFSGKTVALFGLGDQVGYPENF (107)
                          |         |         |         |         |
                         60        70        80        90       100

D. vulgaris     CGAVDAIEEKLKNLGAEIVQD--------------------GLRIDGDP--RAAR (134)
A. nidulans     QDAMGILEEKISSLGSQTVGYWPIEGYDFNESKAVRNNQFVGLAIDEDNQPDLTK (154)
A. chroococcum  LDAMGELHSFFTERGAKVVGAWSTDGYEFEGSTAVVDGKFVGLALDLDNQSGKTD (162)
                  |         |         |         |         |         |
                 110       120       130       140       150       160

D. vulgaris     DDIVGWAHDVRGAI---- (148)
A. nidulans     NRIKTWVSQLKSEFG--L (170)
A. chroococcum  ERVAAWLAQIAPEFGLSL (180)
                          |         |
                         170       180
```

Fig. 1. (A) Nucleotide sequence and deduced amino acid sequence of the *nifF* gene encoding the flavodoxin AcFld2 from *Azotobacter chroococcum*. The putative ribosome binding site for the *nifF* gene is underlined. The sequence is deposited with Genbank with the accession number M73019; (B) sequence alignment of flavodoxins from *Desulfovibrio vulgaris*, *Anacystis nidulans* and *A. chroococcum*. The extra loop, characteristic for long-chain flavodoxins is found in *A. chroococcum* from residue Trp^{129} to Val^{148}. Consensus flavin-binding-site residues in *A. nidulans* flavodoxin are underlined (Stockman et al., 1990).

1991). They all consist of a central parallel β-sheet consisting of five strands, linked by four or five α-helical segments that occur in parallel pairs on the exterior of the molecule. In the obligate aerobe *Azotobacter chroococcum*, flavodoxin-2 acts as an electron donor to nitrogenase (Yates, 1972; Bagby et al., 1991): two-electron-reduced flavodoxin transfers one electron to the dimeric Fe protein of the nitrogenase enzyme complex (Kim and Rees, 1994). After this electron-transfer reaction, the flavodoxin returns to the one-electron-reduced state. The midpoint potential of this semiquinone–hydroquinone couple is −522 mV, which is the most negative redox potential observed for flavodoxins (Deistung and Thorneley, 1986). This potential of −522 mV is almost 400 mV more negative than the midpoint potential of the semiquinone–hydroquinone couple of free FMN, which is −124 mV (Curley et al., 1991). The apoprotein surrounding the FMN is therefore very important in modulating this midpoint potential. Zhou and Swenson (1995) have found that for the flavodoxin from *Desulfovibrio vulgaris* negatively charged amino acid residues located near the FMN binding site contribute to the low midpoint potential of the semiquinone–hydroquinone couple, because the mutation of some of these negatively charged amino acids to neutral residues resulted in an increase of the midpoint potential. Because of the very low semiquinone–hydroquinone midpoint potential of the *A. chroococcum* flavodoxin, it is interesting to investigate if there are more negatively charged residues surrounding the FMN in this flavodoxin than in the flavodoxin from *D. vulgaris*. The *nifF*-encoded flavodoxin from *A. chroococcum* (ACFld2, molecular mass of 20 kDa) contains 180 amino acids and is therefore one of the longer chain flavodoxins (Mayhew and Tollin, 1992), differing from the short-chain ones mainly by an insertion of 20 residues in a loop in the fifth strand of the β-sheet (Fig. 1B; residues 129–148). This flavodoxin is the largest one studied by multidimensional NMR.

The purpose of this study is twofold. Firstly, we wanted to determine the ^{1}H, ^{15}N and ^{13}C backbone with ^{1}H and ^{13}C beta assignments as well as the solution secondary structure of oxidized *A. chroococcum* flavodoxin, by using heteronuclear multidimensional NMR spectroscopy. Knowledge of this secondary solution structure will be the first step in gaining more structural information about this flavodoxin. More structural information is very important in order to understand the unusual low semiquinone–hydroquinone midpoint potential of this flavodoxin. Secondly, we performed an interaction study of the flavodoxin with the Fe protein of the nitrogenase complex, by using NMR. This will gain insight as to which residues are involved in complex formation between flavodoxin and the Fe protein. This information is important for understanding the mechanism of electron transfer from flavodoxin to nitrogenase.

Materials and Methods

Molecular cloning, protein expression and purification of flavodoxin

The flavodoxin-encoding gene for flavodoxin-2 is located on the major nitrogen-fixation (*nif*) gene cluster from *A. chroococcum*. It was located 1.5 kb downstream of the *nifM* gene sequenced earlier (Evans et al., 1991). The entire *nifF* gene on a 1.6-kb *Pst*I fragment was cloned from the recombinant cosmid pACB1 (Jones et al., 1984) into plasmid pEMBL19+ (Dente et al., 1983) to give pMOY10a. The insert was sequenced by the dideoxynucleotide chain-termination method (Sanger et al., 1977) with 5'-[α-^{35}S]dATP (600 Ci'mmol; Amersham International, Little Chalfont, U.K.), sequenase (Amersham International) and 7-deaza-dGTP, instead of dGTP, to eliminate compressions. Sequencing was performed from deletions and completed using oligonucleotide primers. The sequence (Fig. 1A) was compiled using the University of Wisconsin Genetics Computer Group programmes (Deveraux et al., 1985). The sequence shows an open reading frame of 180 amino acid residues with a calculated pI of 4.27. The deduced amino acid sequence for the *A. chroococcum* flavodoxin showed 10 differences and overall 94.4% identity with the sequence of the comparable gene product from *Azotobacter vinelandii* (Bennet et al., 1988). Detailed information about the expression and purification of the flavodoxin is given in the Supplementary Material. After purification, the flavodoxin was concentrated in an Amicon Centripep Concentrator (Amicon Ltd., Stonehouse, U.K.). The final yields were 11 and 173 mg for the ^{13}C,^{15}N-labelled and ^{15}N-labelled flavodoxin, respectively.

The Fe protein of the vanadium–nitrogenase complex from *A. chroococcum* was purified as decribed by Eady et al. (1988).

NMR sample preparation

Four samples were prepared for the NMR experiments. One contained 4.8 mM oxidized flavodoxin, uniformly labelled (> 80%, as determined from a ^{15}N-coupled 1D proton NMR spectrum) with ^{15}N, dissolved in 90% H_2O/10% D_2O, 150 mM potassium pyrophosphate/HCl, pH 6.5, and 0.4 mM TSP. The second sample contained 0.9 mM oxidized flavodoxin, uniformly labelled (> 80%, as determined from a ^{13}C-^{15}N-coupled 1D proton NMR spectrum) with ^{13}C and ^{15}N, dissolved in 90% H_2O/10% D_2O, 150 mM potassium pyrophosphate/HCl, pH 6.5, and 0.4 mM TSP. A third sample for the identification of slowly exchanging amide protons was prepared by lyophilization of 3.8 ml 0.3 mM oxidized flavodoxin, uniformly labelled (> 80%) with ^{15}N, dissolved in 20 mM potassium pyrophosphate/HCl, pH 6.85. The lyophilized flavodoxin was dissolved in 0.5 ml D_2O, giving an NMR sample containing 2.5 mM oxidized flavodoxin, uniformly labelled

(> 80%) with ^{15}N in 150 mM potassium pyrophosphate/HCl, pH 6.5. All samples were evacuated and filled with argon for at least four times. The pH was not corrected for isotope effects. The last sample, which contained 2.5 mM oxidized flavodoxin, uniformly labelled (> 80%) with ^{15}N, dissolved in 90% H_2O/10% D_2O, 150 mM potassium phosphate, pH 7.0, and 0.2 mM TSP, was made anaerobic by five cycles of evacuation and filling with argon. To reduce the flavodoxin to its semiquinone form, an anaerobic sodium dithionite solution was added to a final concentration of about 12 mM.

Titration of flavodoxin with the Fe protein

A sample containing 1.5 mM oxidized flavodoxin, uniformly labelled (> 80%) with ^{15}N, dissolved in 90% H_2O/10% D_2O, 50 mM potassium phosphate, pH 7.1, and 0.4 mM TSP, was made anaerobic by five cycles of evacuation and filling with argon. The purified Fe protein (dimer) of the vanadium nitrogenase complex, dissolved in 50 mM potassium phosphate, pH 7.1, and 1 mM sodium dithionite, was left at room temperature for at least 2 h in order to allow the dithionite to be oxidized by the Fe protein. Since the Fe protein is unstable under aerobic conditions, it is important to work anaerobically. Stock solutions of 0.15 M MgADP at pH 7, and 2 M KCl in 50 mM potassium phosphate, pH 7.1, were made anaerobic by extensive flushing with argon. The oxidized flavodoxin was titrated with the dithionite-free Fe protein, MgADP and KCl under anaerobic conditions as described in the Supplementary Material (Table S1). Two-dimensional ^1H-^{15}N HSQC spectra (Bodenhausen and Ruben, 1980) were recorded for each titration at 25 °C, acquiring 128 real t_1 points (^{15}N; spectral width 1672 Hz), 1024 complex t_2 points (^1H; spectral width 8064 Hz) with 16 scans per t_1 increment, using time-proportional phase incrementation (TPPI) (Marion and Wüthrich, 1983). Presaturation of the water signal was employed during the 1.5-s relaxation delay.

NMR spectroscopy

Unless otherwise stated, all experiments were performed at 30 °C on a Bruker AMX-500 or AMX-600 spectrometer using either a triple-resonance 5-mm inverse probe or a triple-resonance 5-mm inverse probe with a self-shielding z-gradient. Presaturation of the water signal during the 1–1.5-s relaxation delay was employed for the nongradient-enhanced NMR experiments. No presaturation during the 1-s relaxation delay was employed for the gradient-enhanced experiments.

To identify fast and slowly exchanging amide protons, a series of 2D ^1H-^{15}N HSQC experiments was recorded at 25 °C after 0.5 h, 7 h, 53 h and 43 days after dissolving the ^{15}N-labelled flavodoxin in D_2O. For each HSQC experiment 128 real t_1 points (^{15}N; spectral width 1600 Hz), 1024 complex t_2 points (^1H; spectral width 8064 Hz) with 16 scans per t_1 increment, using TPPI, were recorded. Amide protons which could still be observed 53 h after dissolving in D_2O were marked as slowly exchangeable in Fig. 5.

Also 2D ^1H-^{15}N HSQC spectra of ^{15}N-labelled flavodoxin in 90% H_2O/10% D_2O in its oxidized and semiquinone redox states were recorded. For the oxidized flavodoxin 128 complex t_1 points (^{15}N; spectral width 1672 Hz), 1024 complex t_2 points (^1H; spectral width 8064 Hz) with 128 scans per hypercomplex t_1 increment, using States-TPPI (Marion et al., 1989c) were recorded. For the one-electron-reduced flavodoxin, 148 complex t_1 points (^{15}N; spectral width 1672 Hz), 1024 complex t_2 points (^1H; spectral width 8064 Hz) with 16 scans per hypercomplex t_1 increment, using States-TPPI were recorded. Due to the paramagnetic character of the isoalloxazine part of the FMN in the semiquinone redox state, resonances of residues within about 15 Å of this isoalloxazine are broadened to a large extent. For the *A. chroococcum* flavodoxin (at 30 °C and 500 MHz) a theoretical extra line-broadening of 10 Hz can be calculated for the resonance of a proton at a distance of about 15 Å from the paramag-

→

Fig. 2. Pulse sequences for the modified triple-resonance experiments with gradient enhancement: (A) CBCANH; (B) CBCA(CO)NH; and (C) ct-HNCO. Narrow and wide pulses correspond to 90° and 180° flip angles, respectively. The 90° (grey) water flip-back pulse has a Gaussian profile (with a duration of 2.1 ms). Pulses for which the phase is not indicated are applied along the x-axis. The ^1H carrier is positioned at the H_2O frequency (4.71 ppm), the carrier for the $^{13}C^{\alpha\beta}$, $^{13}C^{\alpha}$ and ^{13}CO pulses are positioned at 47, 59 and 176 ppm, respectively. The power of the $^{13}C^{\alpha}$ and $^{13}C^{\alpha\beta}$ pulses is adjusted such that they do not excite the ^{13}CO nuclei. The power of the ^{13}CO pulses are adjusted such that they do not excite the $^{13}C^{\alpha}$ nuclei. The shaped ^{13}CO pulses have an amplitude profile corresponding to the center lobe of a sinc function (with a duration of 202 μs). ^{15}N decoupling is accomplished using GARP modulation with a 2.1-kHz rf field. (A) CBCANH: $\delta = 1.5$ ms; $\varepsilon = 2.4$ ms; $\zeta = 11$ ms; $\xi = 11.4$ ms; $\kappa = 3.2$ ms; $\lambda = 2.65$ ms; $\mu = 1$ ms; $T_{AB} = 3.55$ ms; $T_N = 5.7$ ms and $T'_N = 8.2$ ms. Phase cycling is as follows: $\phi_1 = y$; $\phi_2 = x,-x$; $\psi_1 = x$; $\phi_3 = x,x,-x,-x$; $\phi_4 = -y$; $\psi_2 = -y$; receiver = x,–x,–x,x; (B) CBCA(CO)NH: $\delta = 1.5$ ms; $\varepsilon = 2.4$ ms; $\zeta = 3.9$ ms; $\eta = 4.5$ ms; $\theta = 11.1$ ms; $\xi = 11.4$ ms; $\kappa = 3.2$ ms; $\lambda = 2.65$ ms; $\mu = 1$ ms; $T_{AB} = 3.55$ ms; $T_N = 5.65$ ms and $T'_N = 8.1$ ms. Phase cycling is as follows: $\phi_1 = y$; $\phi_2 = x,-x$; $\psi_1 = x$; $\phi_3 = x,x,-x,-x$; $\phi_4 = 120°$ (Bloch–Siegert phase error compensation); $\phi_5 = -y$; $\psi_2 = -y$; receiver = x,–x,–x,x; (C) ct-HNCO: $\delta = 2.75$ ms; $\lambda = 2.75$ ms; $\mu = 1$ ms; $T_N = 13.75$ ms and $T'_N = 11$ ms; $T''_N = T_N - (t_2/2)$. Phase cycling is as follows: $\phi_1 = y$; $\phi_2 = y,-y$; $\phi_3 = x,-x$; $\psi_1 = x,x,-x,-x$; $\phi_4 = 325°$; $\phi_5 = -x$; $\psi_2 = y$; receiver = x,x,–x,–x. Quadrature detection in t_1 is obtained by changing phase ψ_1 in a States-TPPI manner. For t_2, N- and P-type spectra are recorded interleaved; N-type spectra with the gradient pulses are as shown and $\psi_2 = y$, and P-type spectra with the gradient pulse G_2 are inverted and $\psi_2 = -y$. Pulsed field gradients have a sine-bell shape, with a duration of $G_1 = 1$ ms and $G_2 = 0.5$ ms. Gradient strengths are set to $G_1 = 80$ and $G_2 = 16$, where a gradient strength of 100 corresponds to ca. 60 G/cm at the center of the gradient.

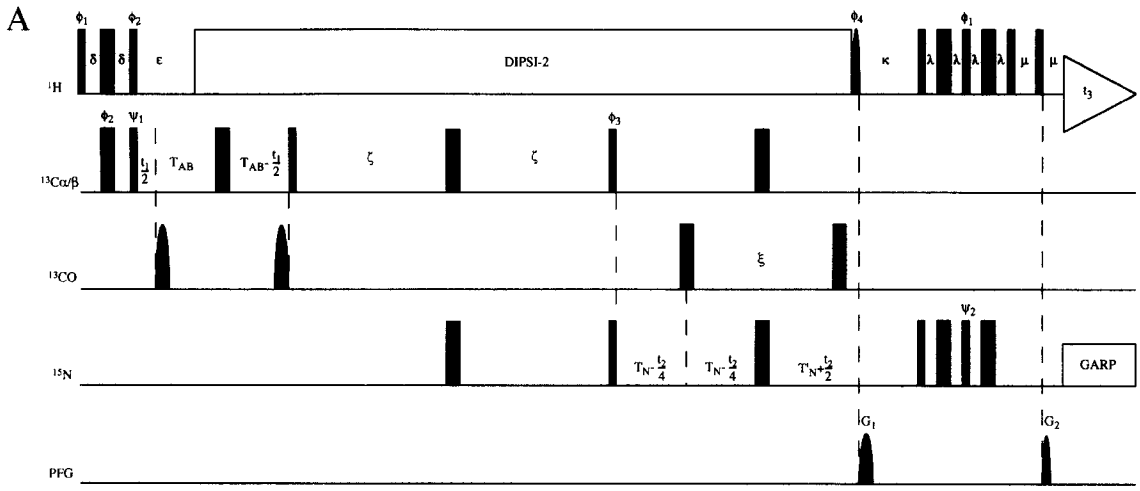
A
DIPSI-2
GARP
PFG

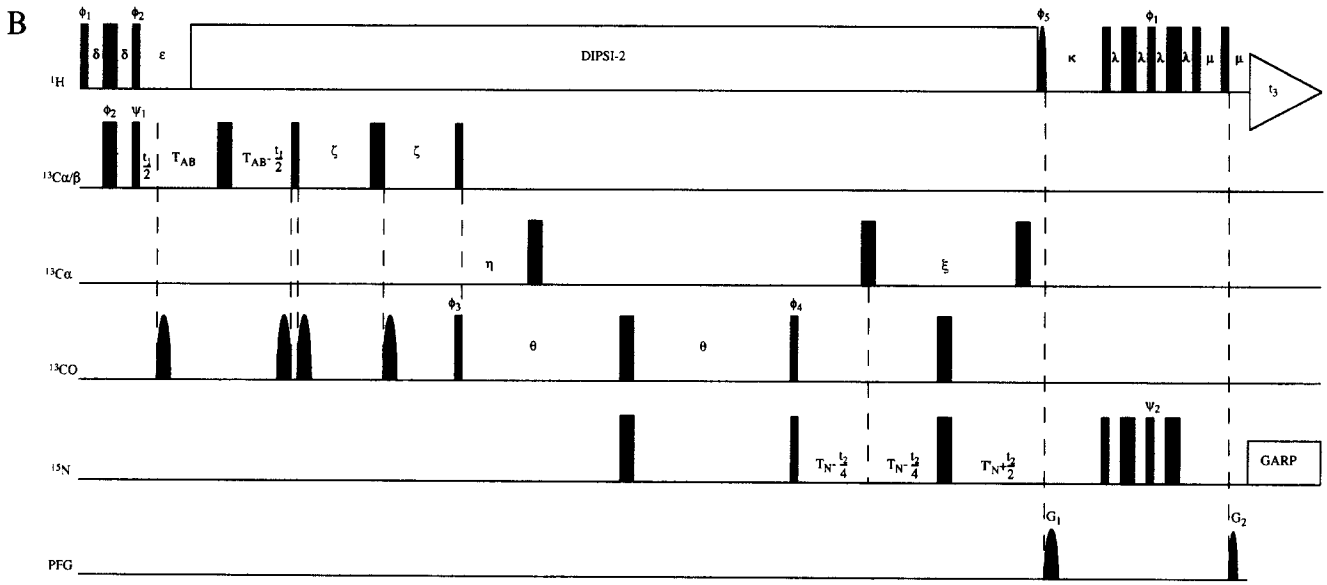
B
DIPSI-2
GARP
PFG

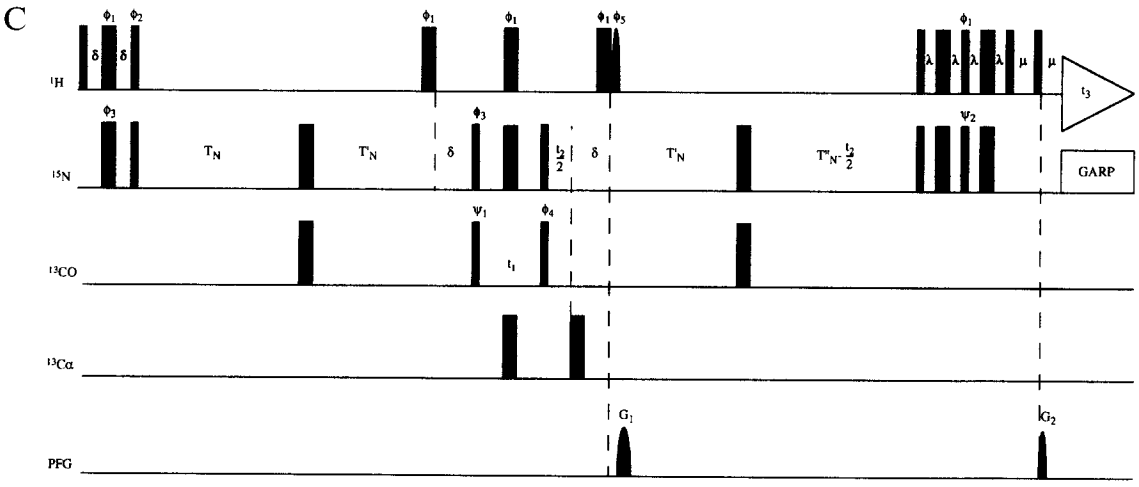
C
GARP
PFG

netic center, by using the Solomon–Bloembergen equation (Solomon, 1955; Bloembergen, 1957). This line-broadening is caused by a dipole–dipole interaction between the proton and the unpaired electron on the isoalloxazine part of the FMN. In this way, residues surrounding to the FMN can be determined. Resonances that became broadened to a large extent are marked as 'SQ-affected' in Fig. 5.

The following 3D experiments were recorded with the 4.8-mM ^{15}N-labelled flavodoxin sample: two 3D ^{15}N-separated NOESY-HMQC (Marion et al., 1989a; Zuiderweg and Fesik, 1989) experiments with NOE mixing times of 75 and 100 ms; and a 3D ^{15}N-separated TOCSY-HMQC (Marion et al., 1989a) experiment, changed to incorporate two different mixing times of 30 and 50 ms, respectively, using the clean-MLEV-17 (Bax and Davis, 1985; Griesinger et al., 1988) mixing sequence surrounded by trim pulses, was recorded. To resolve NOE cross-peaks of degenerate amide protons, a 3D ^{15}N-separated HMQC-NOESY-HMQC (Frenkiel et al., 1990; Ikura et al., 1990) experiment with a NOE mixing time of 75 ms was recorded. A 3D HNHA experiment (Vuister and Bax, 1993) was recorded for measuring $^{3}J_{H^{N}H^{\alpha}}$ coupling constants. Homonuclear de- and rephasing delays according to Vuister and Bax (1993) were used. In combination with the HAHB(CO)NH experiment (Grzesiek and Bax, 1993) the HNHA was also used for the sequential assignment (Vuister et al., 1994). Determination of the $^{3}J_{H^{N}H^{\alpha}}$ coupling constants was done according to Vuister and Bax (1993), using a correction factor of 1.1.

For the 0.9-mM ^{13}C,^{15}N-labelled flavodoxin sample, the original 3D triple-resonance experiments were modified to incorporate Cavanagh–Rance–Kay gradient enhancement (Cavanagh and Rance, 1990; Cavanagh et al., 1991; Palmer III et al., 1991; Kay et al., 1992) according to Kay et al. (1992). To minimize signal loss, the water signal is returned to its equilibrium position before the start of the acquisition (Stonehouse et al., 1994) by a selective Gaussian water flip-back pulse. The present implementation is a simplification of the one suggested by Stonehouse et al. (1994), in that only one selective pulse is required. Figure 2 shows three of the modified pulse sequences, which are representative for all triple-resonance experiments used in this study: the CBCANH experiment (Grzesiek and Bax, 1992a; Fig. 2A), the CBCA(CO)NH experiment (Grzesiek and Bax, 1992b; Fig. 2B) and the ct-HNCO experiment (Grzesiek and Bax, 1992c; Jahnke and Kessler, 1994; Fig. 2C). For the sequential assignment a ct-HNCA experiment (Grzesiek and Bax, 1992c; Jahnke and Kessler, 1994) and a HBHA(CO)NH experiment (Grzesiek and Bax, 1993) were also recorded. The ct-HNCA experiment is similar to the ct-HNCO experiment (Fig. 2C), except for the fact that the ^{13}CO and $^{13}C^{\alpha}$ frequency labels in Fig. 2C are interchanged. The HBHA(CO)NH experiment is identical to the CBCA(CO)NH experiment in Fig. 2B, except for the part up to the first ζ-delay. This part was recorded as given by Grzesiek and Bax (1993). Quadrature detection in the t_1 dimension of all 3D experiments and in the t_2 dimension of the nonenhanced 3D experiments was obtained by using the States-TPPI acquisition scheme (Marion et al., 1989c). Quadrature detection in the t_2 dimension (^{15}N) of the triple-resonance experiments was obtained by alternate N- and P-type selection (Cavanagh et al., 1991; Kontaxis et al., 1994). Additional details regarding acquisition parameters of the 3D NMR experiments are given in Table 1.

NMR processing and data analysis

The spectra were processed on a Silicon Graphics IndigoII workstation using FELIX 2.3 (Biosym, San Diego, CA). For processing States-TPPI and P/N-type spectra macros (written in-house) were used. The data were apodized in the acquisition dimension using a Gaussian multiplication with a line-broadening of −7 Hz and a Gaussian multiplication factor of 0.1, before zero-filling to 1024 real points for the 3D spectra and 2048 real points for the 2D spectra. For the indirectly detected dimensions the data were apodized using a squared co-

TABLE 1
ACQUISITION PARAMETERS FOR THE 3D NMR EXPERIMENTS

Experiment	Nucleus			Number of complex points			Spectral width (Hz)			Scans per hypercomplex t_1/t_2 increment
	t_1	t_2	t_3	t_1	t_2	t_3	t_1	t_2	t_3	
^{15}N-NOESY-HMQC	^{1}H	^{15}N	^{1}H	128	45	512	8064	1672	8064	16
^{15}N-TOCSY-HMQC	^{1}H	^{15}N	^{1}H	128	48	512	8064	1672	8064	32
HMQC-NOESY-HMQC	^{15}N	^{15}N	^{1}H	64	38	512	1672	1672	8064	64
HNHA	^{1}H	^{15}N	^{1}H	47	24	512	5580	2068	9615	64
CBCANH	$^{13}C^{\alpha\beta}$	^{15}N	^{1}H	64	48	512	10 000	2235	9615	40
CBCA(CO)NH	$^{13}C^{\alpha\beta}$	^{15}N	^{1}H	64	48	512	10 000	2235	9615	16
ct-HNCO	^{13}CO	^{15}N	^{1}H	50	55	512	1502	2008	9615	8
CBCANH	$^{13}C^{\alpha}$	^{15}N	^{1}H	50	52	512	1502	2008	9615	16
HBHA(CO)NH	$^{1}H^{\alpha\beta}$	^{15}N	^{1}H	64	44	512	4316	2235	9615	40

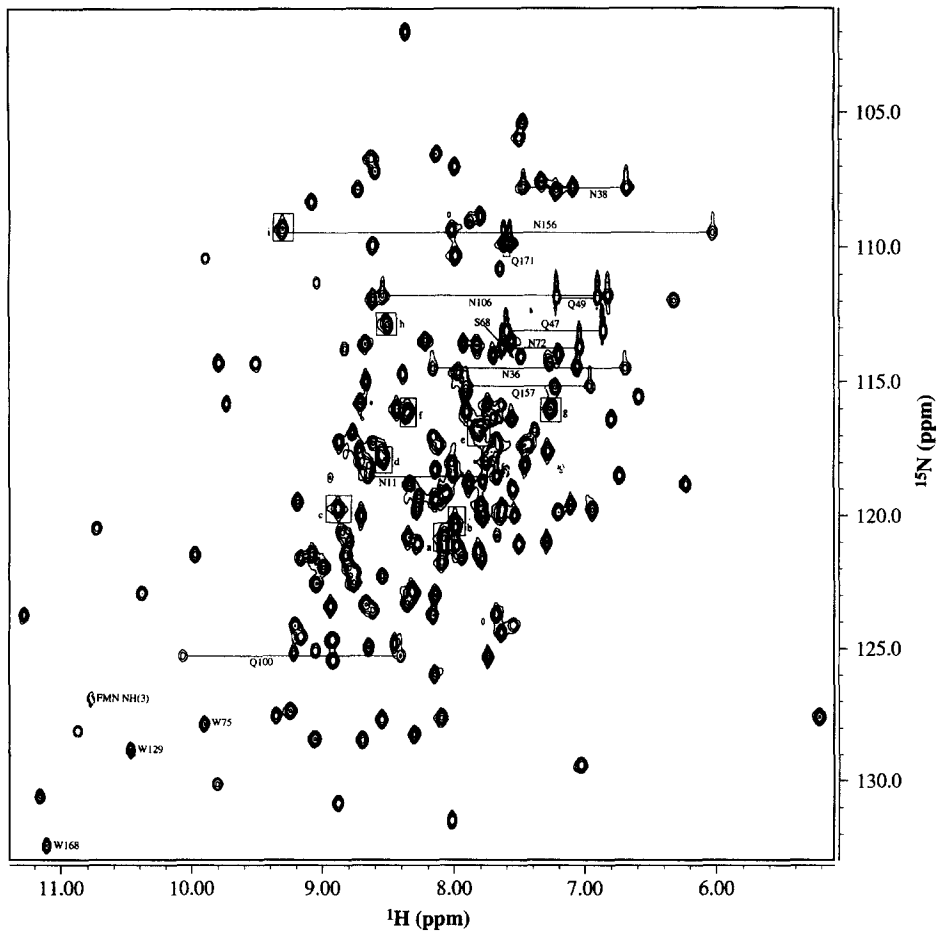

Fig. 3. 2D ^{1}H-^{15}N HSQC spectrum of 4.8 mM oxidized *Azotobacter chroococcum* flavodoxin. Cross-peaks of the Asn and Asp side-chain amino groups are labelled, as are the Trp indole NH correlations. The aliased FMN NH(3) cross-peak, as well as the amide cross-peak of Ser^{68}, are labelled too. Negative resonances are marked by dashed contours. ^{1}H-^{15}N cross-peaks which consist of two or three resonances are marked by rectangles: a (Val^{37}, Phe^{45}, Lys^{90}); b (Thr^{91}, Ala^{167}); c (Leu^{63}, Glu^{137}); d (Asp^{28}, Ser^{88}, Ser^{116}); e (Ser^{21}, Leu^{79}); f (Ala^{46}, Glu^{73}); g (Tyr^{103}, Met^{111}); h (Ser^{10}, Thr^{131}); and i (Gly^{102}, $Asn^{156}(N^{\delta}H^{\delta})$).

sine-bell window function. After the apodization the data were zero-filled to the next power of 2, Fourier-transformed and phased. A FLATT baseline correction (Güntert and Wüthrich, 1992) was applied to F_1 of the ^{15}N-separated TOCSY- and NOESY-HMQCs and to the F_2 dimension of the 2D ^{1}H-^{15}N HSQCs. Solvent suppression by convolution of the time domain data (Marion et al., 1989b) in the acquisition dimension was applied to the 3D triple-resonance spectra and to the ^{15}N-separated TOCSY-HMQC. The data were analyzed using the program XEASY (ETH, Zürich, Switzerland; Bartels et al., 1995). A consensus chemical shift index for assigning protein secondary structure, was calculated using the Chemical Shift Index program (Wishart et al., 1992; Wishart and Sykes, 1994). ^{1}H chemical shifts were referenced using internal TSP as a standard. TSP was set to –0.014 ppm, which is the pH-corrected chemical shift value when DSS is set to 0 ppm. ^{15}N and ^{13}C chemical shifts were referenced indirectly using the following, temperature-corrected, Ξ-values of 0.251449533 and 0.101329118 for ^{13}C and ^{15}N, respectively (Wishart et al., 1995).

Results

Figure 3 shows a 2D ^{1}H-^{15}N HSQC spectrum of uniformly ^{15}N-labelled *A. chroococcum* flavodoxin in the oxidized form. For a protein of 180 amino acids the dispersion of the ^{1}H-^{15}N cross-peaks is rather good. Nevertheless, some cross-peaks in Fig. 3 are composed of two or three overlapping ^{1}H-^{15}N resonances (boxed regions): a (Val^{37}, Phe^{45}, Lys^{90}); b (Thr^{91}, Ala^{167}); c (Leu^{63}, Glu^{137}); d (Asp^{28}, Ser^{88}, Ser^{116}); e (Ser^{21}, Leu^{79}); f (Ala^{46}, Glu^{73}); g (Tyr^{103}, Met^{111}); h (Ser^{10}, Thr^{131}); and i (Gly^{102}, $Asn^{156}(N^{\delta}H^{\delta})$). All these degeneracies, however, could be resolved in a 3D ct-HNCO experiment. Out of a total of 175 non-proline residues, 172 ^{1}H-^{15}N amide cross-peaks could be observed. The only amide cross-peaks missing are the ones from Ala^{2} and Gly^{159}. Flavodoxin from *A. chroococcum* contains six asparagines, five glutamines and three tryptophans. Cross-peaks of all 11 side-chain amino groups of the asparagines and glutamines, as well as the three indole NH groups of the tryptophans, are observed in the ^{1}H-^{15}N HSQC spectrum (Fig. 3). Be-

sides, ^{1}H-^{15}N cross-peaks from the apoprotein, and one cross-peak from the FMN, i.e. NH(3), are observed. All these cross-peaks are indicated in Fig. 3. The FMN NH(3) ^{1}H and ^{15}N frequencies resonate at 10.77 and 159.9 ppm, respectively; the ^{1}H-^{15}N cross-peak is therefore aliased in the ^{15}N dimension of the spectrum shown in Fig. 3. The ^{1}H-^{15}N cross-peaks of the backbone amides are not labelled to prevent Fig. 3 from becoming too crowded; their chemical shifts are listed in the Supplementary Material (Table S2).

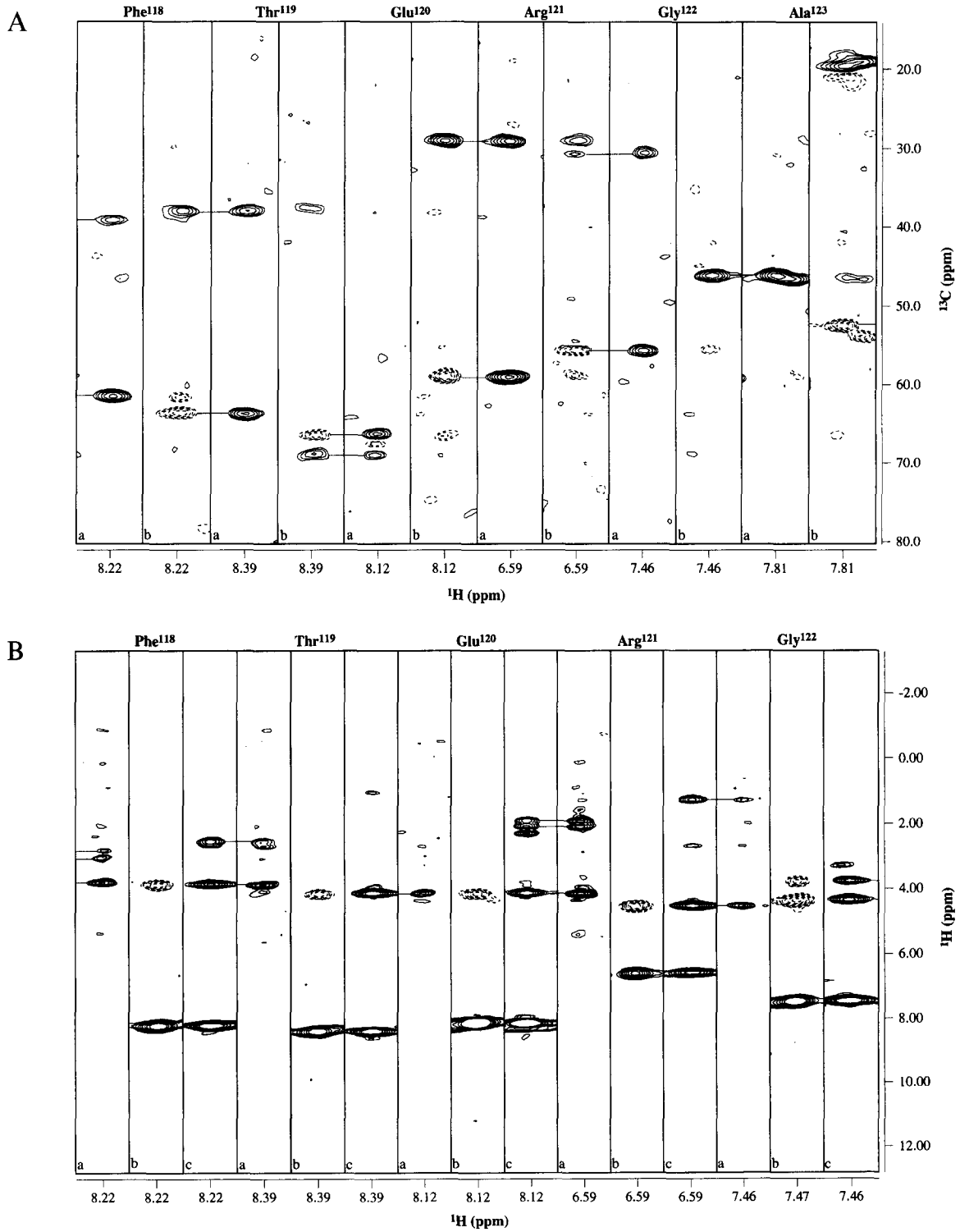

Fig. 4. (A) Strips along the ^{13}C axes of the (a) CBCA(CO)NH and (b) CBCANH spectra taken at the ^{1}H-^{15}N resonance frequencies of Phe^{118}–Ala^{123} showing sequential connectivities; (B) Strips along the ^{1}H axes of the (a) HBHA(CO)NH, (b) HNHA and (c) ^{15}N-TOCSY-HMQC spectra taken at the ^{1}H-^{15}N resonance frequencies of Phe^{118}–Gly^{122} showing sequential connectivities. Resonances of negative intensity are marked by dashed contours.

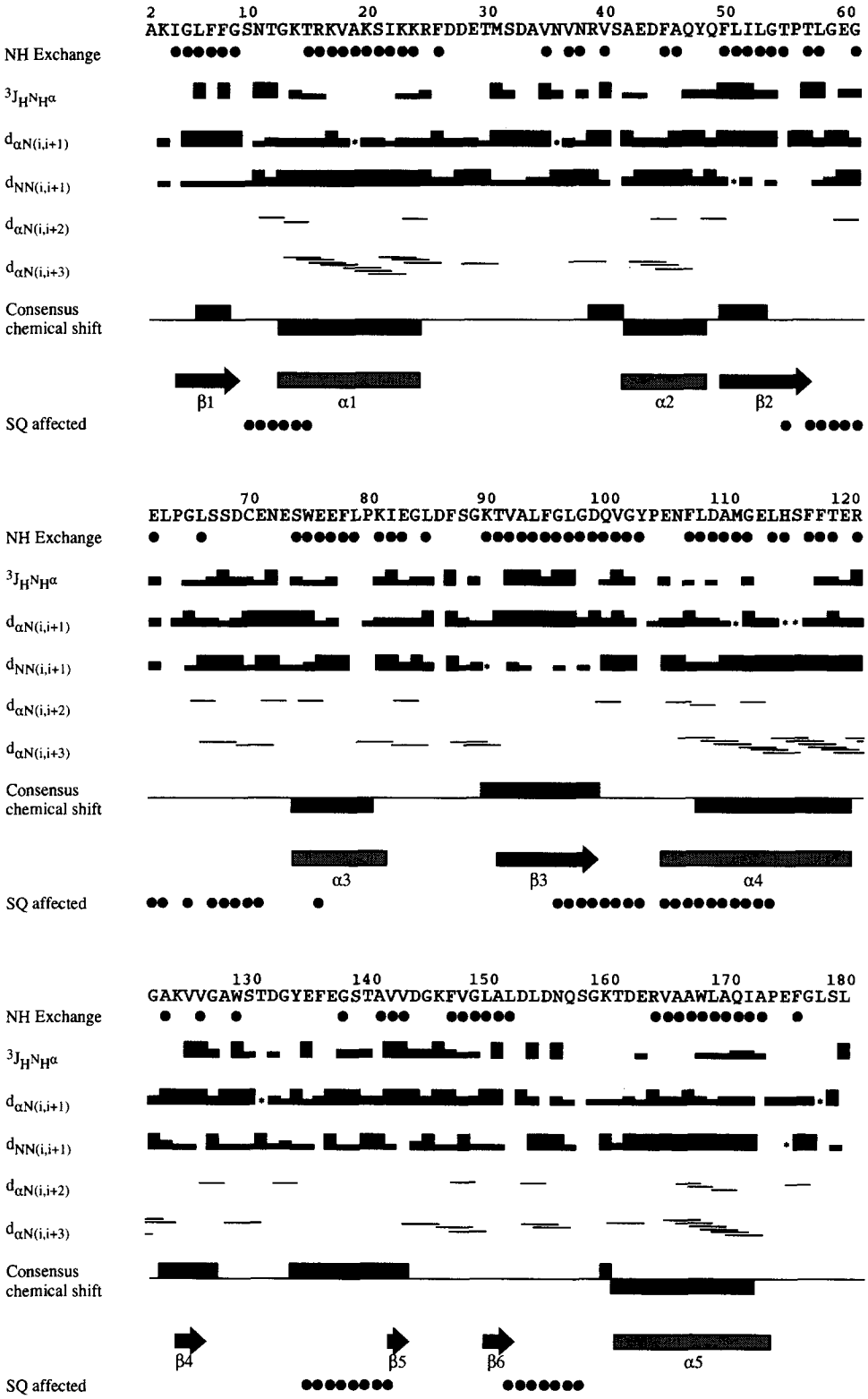

Fig. 5. Summary of the NMR data obtained for oxidized *Azotobacter chroococcum* flavodoxin on amide-proton exchange, sequential and medium-range NOE connectivities, $^3J_{H^N H^\alpha}$ coupling constants, $^1H^\alpha$, $^{13}C^\alpha$, $^{13}C^\beta$ and ^{13}CO secondary shifts depicted as consensus chemical shifts, the secondary structure elements deduced from these data and the amide protons broadened by the one-electron-reduced FMN. Amide protons which are still observed 53 h after dissolving lyophilized flavodoxin in D_2O in a 2D ^1H-^{15}N HSQC spectrum are marked by dots. $^3J_{H^N H^\alpha}$ coupling constants as determined from the HNHA experiment are given by black and shaded boxes for nonoverlapping and sligthly overlapping resonances, respectively. Large boxes: $^3J_{H^N H^\alpha} > 8$ Hz; medium-sized boxes: 5 Hz $< {}^3J_{H^N H^\alpha} < 8$ Hz; small boxes: $^3J_{H^N H^\alpha} < 5$ Hz. Strong, medium and weak sequential NOE connectivities are indicated by large, medium-sized and small boxes. Shaded boxes denote partial overlap and stars denote uncertain connectivities due to overlap. Consensus chemical shift: Positive and negative boxes denote chemical shift derived β-sheet and α-helix conformations, respectively. Residues of which the amide protons are affected by the one-electron-reduced FMN are indicated by dots.

Sequential assignments

The sequential assignments were achieved through the use of the CBCANH experiment in combination with the CBCA(CO)NH experiment and the combined use of the ^{15}N-TOCSY-HMQC, HNHA and HBHA(CO)NH experiments. The assignment started by picking all amide peaks in a 2D ^{1}H-^{15}N HSQC spectrum. The picked peaks were transferred to a 3D ct-HNCO spectrum in order to resolve overlapping resonances. The ^{1}H and ^{15}N frequencies of the picked peaks in the ct-HNCO spectrum next were transferred to the CBCANH spectrum and adjusted to the corresponding intraresidue $^{13}C^{\alpha}$ and $^{13}C^{\beta}$ resonances by making use of the CBCA(CO)NH spectrum. Analogously, the ^{1}H-^{15}N frequencies of the picked ct-HNCO peaks were transferred to the HNHA and ^{15}N-TOCSY-HMQC spectra and adjusted to the intra-residual $^{1}H^{\alpha}$ and $^{1}H^{\beta}$ resonances, using the HBHA(CO)NH spectrum. Next, spin system information was obtained from the ^{15}N-TOCSY-HMQC, as described by Wüthrich (1986). Due to the size of *A. chroococcum* flavodoxin it was not possible to assign all spin systems, but those that were assigned were categorized in the following classes: Gly, Ala, Val, AMX and long-chain. Thanks to their characteristic $^{13}C^{\alpha}$ and $^{13}C^{\beta}$ chemical shift values, Gly, Ala and Ser/Thr could be assigned from the CBCANH/CBCA(CO)NH experiments (Grzesiek and Bax, 1993). Cross-peaks of $^{13}C^{\alpha}$ resonances of Ser and Thr, which overlap with their intraresidual $^{13}C^{\beta}$ resonance, are not observed in a CBCANH experiment because they cancel one another due to their opposite signs. In this case the ct-HNCA experiment was used to determine the $^{13}C^{\alpha}$ resonance. Gly and Ala were used as starting points in the sequential assignment using the CBCANH and CBCA(CO)NH spectra. In this way, stretches of sequential residues were obtained, which is illustrated in Fig. 4A. In this figure strips are shown along the ^{13}C axes of the CBCANH and CBCA(CO)NH spectra taken at the ^{1}H-^{15}N resonance frequencies of Phe^{118}-Ala^{123}. In combination with the spin-system information these stretches were mapped onto the primary sequence. Ambiguities as to what the next sequential neighbour will be, cause the stretch to end. However, if a stretch can be mapped uniquely onto the primary sequence, $^{13}C^{\alpha}$ and $^{13}C^{\beta}$ chemical shift information (Grzesiek and Bax, 1993) of residue n-2 can be used to identify which of the degenerate n-1 candidates is the correct one. In this way, almost all amide resonances could be sequentially assigned. Ambiguities in the CBCANH/CBCA(CO)NH-based assignments were solved by assignments based on the HNHA and ^{15}N-TOCSY-HMQC in combination with the HBHA(CO)NH spectra. An example of the sequential assignment based on these three experiments is given in Fig. 4B. This combination of experiments also served as a check for the assignments obtained from the CBCANH and CBCA(CO)NH spectra. Furthermore, it yielded the chemical shifts of the $^{1}H^{\alpha}$ and $^{1}H^{\beta}$ protons. Finally, the ^{13}CO chemical shifts were determined from the ct-HNCO spectrum. A list of the chemical shifts of $^{1}H^{N}$, ^{15}N, $^{13}C^{\alpha}$, $^{1}H^{\alpha}$, $^{13}C^{\beta}$, $^{1}H^{\beta}$ and ^{13}CO de-

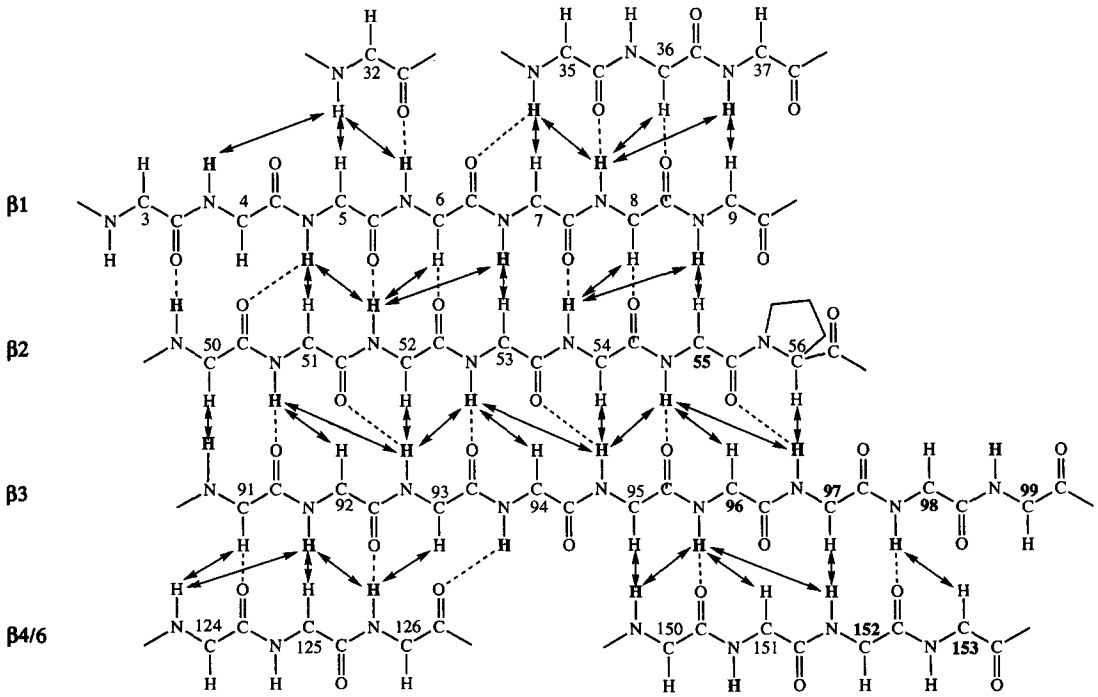

Fig. 6. Topology of central β-sheet of *Azotobacter chroococcum* flavodoxin. Interstrand long-range NOE connectivities are indicated by double arrows. Slowly exchangeable amide protons are in bold lettertype. Hydrogen bonds, as expected on the basis of NOEs and slow amide proton exchange, are indicated by dashed lines. Amide protons of residues of which the residue-number is in bold lettertype are affected by the one-electron-reduced FMN.

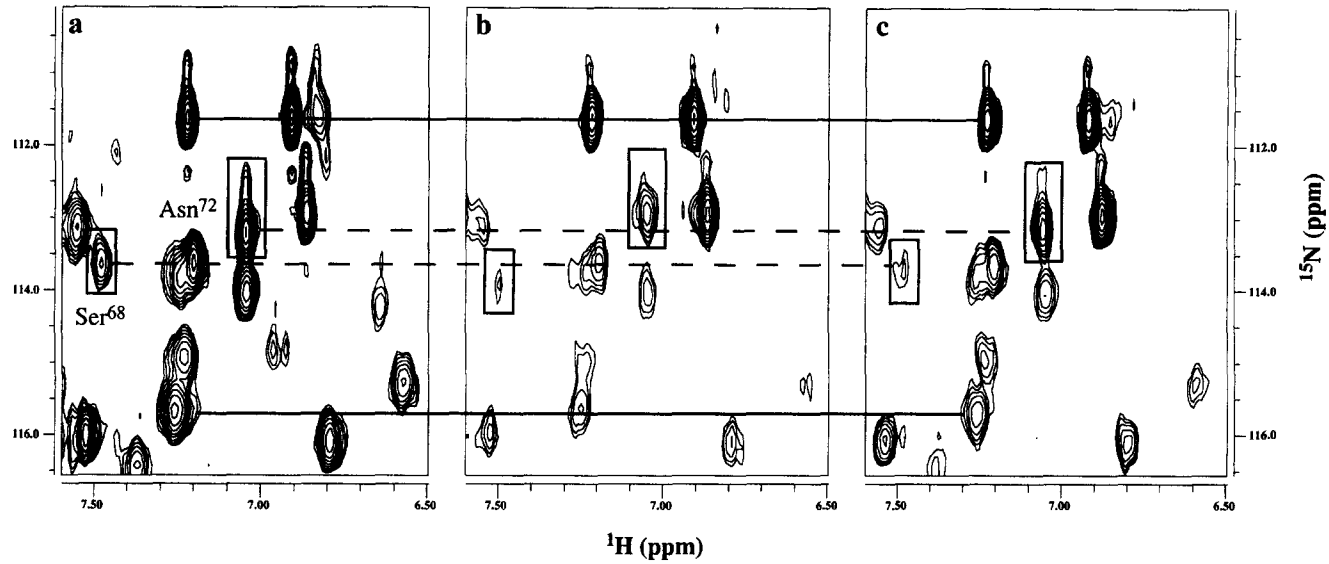

Fig. 7. Parts of ^{15}N-HSQC spectra of *Azotobacter chroococcum* flavodoxin at pH 7.1, 25 °C. (a) 1.5 mM flavodoxin; (b) 0.96 mM flavodoxin; and 0.96 mM Fe protein; and (c) as in (b), with 96 mM KCl and 2.7 mM MgADP. The amide resonance of Ser^{68} and the amino side-chain resonance of Asn^{72}, for which a chemical shift change is observed, are marked by rectangles. Three other resonances, the amino side-chain resonances of Gln^{49} and the degenerate amide resonances of Tyr^{103} and Met^{111}, are marked by solid lines for comparison.

rived from these experiments, is given in the Supplementary Material (Table S2).

The ^{1}H-^{15}N cross-peaks in the HSQC spectrum of the side-chain amino groups of Asn and Gln were assigned by comparing the TOCSY and NOESY ladders correlated to the backbone amide proton with those correlated to the side-chain amino protons. The ^{1}H-^{15}N cross-peaks in the HSQC spectrum of the indole NHs were assigned on the basis of observed NOEs between the Trp β-protons with the intraresidual indole NH proton in a ^{15}N-NOESY-HMQC spectrum.

Secondary structure

The solution secondary structure was determined from NOE connectivity patterns, amide proton exchange, $^{3}J_{H^N H^\alpha}$ coupling constants (Wüthrich, 1986) and $^{1}H^{\alpha}$, $^{13}C^{\alpha}$, $^{13}C^{\beta}$ and ^{13}CO chemical shifts (Wishart et al., 1992; Wishart and Sykes, 1994). These data and the secondary structure elements derived from them are shown in Fig. 5. The NOE connectivity patterns were obtained from the ^{15}N-NOESY-HMQC and the HMQC-NOESY-HMQC experiments, the $^{3}J_{H^N H^\alpha}$ couplings from the HNHA experiment, and the amide-proton exchange from 2D ^{1}H-^{15}N HSQC experiments in D_2O. Instead of displaying secondary chemical shift values, the calculated consensus chemical shift (Wishart and Sykes, 1994) is given in Fig. 5. In combination with the chemical shift information, helical regions are characterized by the presence of $d_{\alpha N(i,i+3)}$, $d_{\alpha N(i,i+2)}$, strong or medium $d_{\alpha N(i,i+1)}$ and strong $d_{NN(i,i+1)}$ NOE connectivities, as well as by small $^{3}J_{H^N H^\alpha}$ (< 5 Hz) coupling constants (Wüthrich, 1986). By contrast, extended conformations are characterized by strong $d_{\alpha N(i,i+1)}$ and weak $d_{NN(i,i+1)}$ NOE connectivities and the absence of $d_{\alpha N(i,i+2)}$ and $d_{\alpha N(i,i+3)}$ NOE connectivities, as well as by large $^{3}J_{H^N H^\alpha}$ (> 8 Hz) coupling constants (Wüthrich, 1986). Five helical regions can be observed: α1(Gly^{13}–Lys^{24}), α2(Ala^{42}–Tyr^{48}), α3(Ser^{74}–Lys^{81}), α4(Glu^{105}–Glu^{120}) and α5(Thr161–Ala^{173}). In Fig. 5 only those $d_{\alpha N(i,i+2)}$ and $d_{\alpha N(i,i+3)}$ NOE connectivities which did not show overlap with other sequential NOE connectivities are indicated. Due to overlap in the HNHA spectrum, $^{3}J_{H^N H^\alpha}$ coupling constants from only 96 out of 175 non-proline residues could be determined. Between the extended conformations several strong $d_{\alpha N(i,j)}$ and medium $d_{NN(k,l)}$ interstrand NOE connectivities could be identified, indicating that these strands form a parallel β-sheet. Besides interstrand long-range NOE connectivities, strong connectivities are also observed between strand β1 and residues 32–37. These observed long-range (interstrand) NOE connectivities are given in Fig. 6. The small extended conformation β5 is not part of the β-sheet, because no long-range interstrand NOE connectivities could be observed. Due to the large number of hydrogen bonds in secondary structure elements, a large number of slowly exchangeable amide protons are observed for these secondary structure elements (Fig. 5). For the central β-sheet these slowly exchangeable amide protons and their most probable hydrogen-bond acceptor are indicated in Fig. 6.

Figure 5 also shows the residues of which the amide-proton resonance is broadened by the paramagnetic FMN of the flavodoxin in the one-electron-reduced redox state. These residues are therefore closely located to the isoalloxazine part of the FMN (within about 15 Å). From this and Fig. 6 it can be concluded that the FMN ring is located at the C-terminal part of the strands β2, β3 and β6. Furthermore, it is observed that residues Glu^{135},

Phe[136], Ser[139] and Val[142] are only slightly affected by the paramagnetic FMN, meaning that this part of the protein is located further away from the isoalloxazine ring.

Titration of flavodoxin with Fe protein

The titration of oxidized ^{15}N-labelled flavodoxin with dimeric Fe protein (molecular mass of 60 kDa for the homodimer), as indicated in the Supplementary Material (Table S1), was monitored by recording 2D ^{1}H-^{15}N HSQC spectra after each titration. The intensities of the ^{1}H-^{15}N correlations in these spectra decrease with increasing Fe-protein/flavodoxin ratio (Fig. 7). Partly, this is an effect of dilution of the sample as more Fe protein is added, but it is also caused by complexation of the flavodoxin with the Fe protein, forming an 80-kDa complex (assuming a 1:1 stoichiometry). Complexation will cause broadening of the ^{1}H-^{15}N resonances of the flavodoxin, and thus a decreased ^{1}H-^{15}N cross-peak intensity. Upon addition of 96 mM KCl, the intensities, despite the extra dilution, again increase, indicating that more uncomplexed flavodoxin is present in the NMR sample (Fig. 7). Besides these changes in intensities, hardly any significant changes in chemical shifts were detected during the titration (Fig. 7, solid lines), except for three residues. Small but significant chemical shift changes for the backbone amide ^{15}N atom of Ser[68] and the side-chain amino ^{15}N atoms of Asn[72] (Fig. 7) and Asn[11] (Fig. 8) were observed during the titration. No significant chemical shift changes for the corresponding protons were observed. For the one-electron-reduced flavodoxin from *Klebsiella pneumoniae* it was found that a stronger complex with its Fe protein is formed when MgADP was present (Thorneley and Deistung, 1988). MgADP was therefore added at the end of the Fe-protein titration series. For the complexation of oxidized flavodoxin with the Fe protein of *A. chroococcum*, MgADP also has an effect on the complex formation, as chemical shift changes of the above-mentioned resonances are observed upon addition of MgADP (Fig. 8). An increase in ionic strength by addition of KCl causes the chemical shifts to shift towards their uncomplexed chemical shift values (Figs. 7 and 8).

Discussion

This study reports the ^{1}H, ^{15}N and ^{13}C backbone and ^{1}H and ^{13}C beta resonance assignments of the flavodoxin-2 from *A. chroococcum*. To date this is the largest flavodoxin studied by 2D and 3D heteronuclear NMR techniques. The NMR data (Fig. 5) indicate that, like other flavodoxins, *A. chroococcum* flavodoxin contains a central parallel β-sheet linked by α-helices, probably folded in an α/β doubly wound superfold (Orengo et al., 1994). All the flavodoxin structures known thus far have a five-stranded central parallel β-sheet. Although the central β-sheet of *A. chroococcum* flavodoxin also consists of five strands, one outer strand (Ser[32]-Val[37]) has no regular-extended conformation, as deduced from the NMR data. Especially the secondary chemical shifts and the presence of some medium-sized $^{3}J_{H^{N}H^{\alpha}}$ coupling constants give an indication of deviation from a regular-extended conformation. However, in view of the observed long-range NOEs to strand β1 (Fig. 6), the stretch Ser[32]-Val[37] can still be considered as a part of the central β-sheet. Besides long-range NOEs, strong sequential $d_{\alpha N(i,i+1)}$ NOEs, indicative for β-sheet

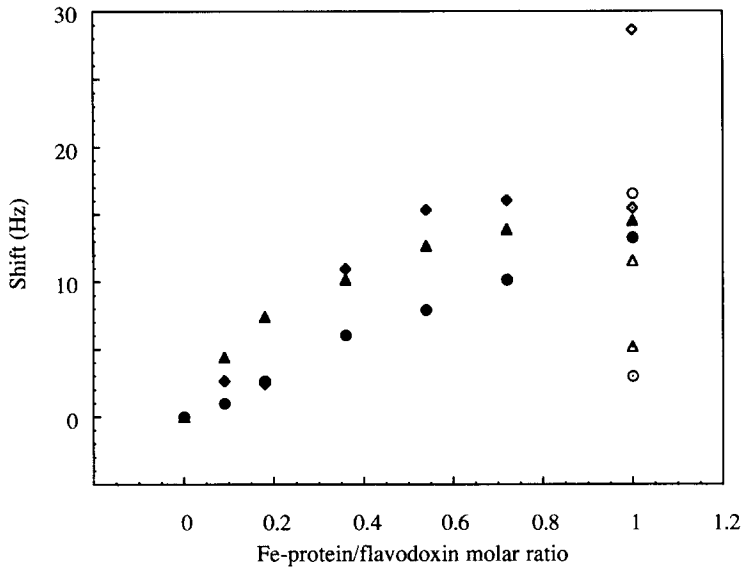

Fig. 8. Absolute ^{15}N chemical shift changes as a function of the Fe-protein/flavodoxin ratio at 25 °C, pH 7.1. The chemical shifts of the uncomplexed flavodoxin are taken as a reference. ◆: side-chain amino group of Asn[11]; ▲: amide group of Ser[68]; ●: side-chain amino group of Asn[72]. Open symbols denote the sample containing 2.8 mM MgADP and open symbols with a dot denote the sample containing 96 mM KCl (and 2.7 mM MgADP).

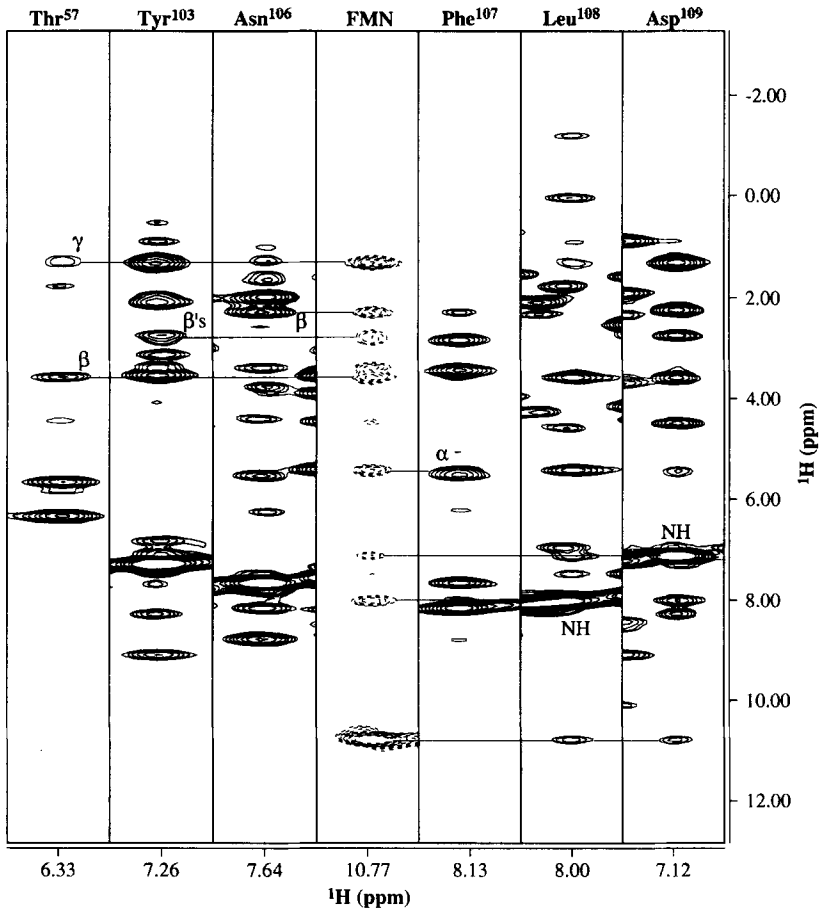

Fig. 9. Strips along the ^{1}H axis of the ^{15}N-NOESY-HMQC spectrum taken at the ^{1}H-^{15}N resonance frequencies of Thr[57], Tyr[103], Asn[106]–Asp[109] and FMN NH(3), showing NOE connectivities between these amino acids and the FMN NH(3) proton. Resonances of negative intensity are marked by dashed contours.

conformation, are also observed in this stretch. Furthermore, the absence of interstrand NOEs between residues Asp[33], Ala[34] and strand β1, is an indication for the irregularity of this stretch. The second outer strand also shows an irregularity, in that this strand is composed of two sequential stretches, Lys[124]-Val[126] and Leu[150]-Leu[152], connected to each other by a loop region. This region contains the residues which form the extra loop in the long-chain flavodoxins. Furthermore, no β-sheet consensus chemical shifts for strand β6 are observed. This means that either this strand also has an irregular-extended conformation, or that the strand is too short to be identified by the CSI program as β-sheet. From Fig. 5 it can be seen that the consensus chemical shift is a good indication for the secondary structure elements in the flavodoxin from *A. chroococcum*. Especially helical structures determined from the consensus chemical shifts are in good agreement with NOEs and $^{3}J_{H^{N}H^{\alpha}}$ coupling constants characteristic for α-helices. For the determination of the β-sheet in this flavodoxin, the consensus chemical shifts perform less well. The strands β1 to β5 are characterized by a β-sheet consensus chemical shift, however, the termination of these strands, as determined by the absence of strong sequential $d_{\alpha N(i,i+1)}$ and weak $d_{NN(i,i+1)}$ NOE connectivities and large coupling constants, differs from the termination on the basis of consensus chemical shifts. Based on former characteristics, the following extended conformations were determined for the flavodoxin from *A. chroococcum* (Fig. 5): β1(Ile[4]–Gly[9]), β2(Phe[50]–Thr[57]), β3(Thr[91]–Asp[99]), β4(Lys[124]–Val[126]), β5(Val[142]–Val[143]) and β6(Leu[150]–Leu[152]). The absense of long-range NOEs between strand β5 and the central β-sheet shows that strand β5 is not part of this sheet. No long-range NOE connectivities between strand β5 and any other part of the protein could be detected. The only NOEs observed were medium-range NOEs between the amide protons of Val[143] and Lys[146], and between the α-proton of Val[142] and the amide protons of Lys[146] and Phe[147]. This indicates the presence of a reverse-turn-like structure in that part of the protein.

Helices were characterized by the presence of $d_{\alpha N(i,i+3)}$, $d_{\alpha N(i,i+2)}$, strong or medium $d_{\alpha N(i,i+1)}$ and strong $d_{NN(i,i+1)}$ NOE connectivities, as well as by small $^{3}J_{H^{N}H^{\alpha}}$ (< 5 Hz) coupling constants. In combination with the consensus chemical shifts, five helical regions were determined: viz., α1(Gly[13]–Lys[24]), α2(Ala[42]–Tyr[48]), α3(Ser[74]–Lys[81]),

α4(Glu^{105}–Glu^{120}) and α5(Thr^{161}–Ala^{173}). Helices α1, α2 and α5 show all the characteristics of a regular α-helix (it has to be borne in mind that not every $d_{\alpha N(i,i+3)}$ connectivity could be assigned, due to overlap). Figure 5 only shows the unambiguously assigned $d_{\alpha N(i,i+3)}$ NOEs. Helices α3 and α4 show some deviation from a regular α-helix. The deviations for helix α3 are found in the N-terminal part of the helix, where some weak $d_{NN(i,i+1)}$ NOE connectivities are observed. The fact that hardly any $d_{\alpha N(1,1+3)}$ NOE connectivities are indicated for this helix in Fig. 5, merely arises from extensive overlap in this region. For helix α4 some medium-sized $d_{NN(i,i+1)}$ NOEs, followed by a weak $d_{\alpha N(i,i+1)}$ NOE can be observed for residues Phe^{107}–Ala^{110}. This part, therefore, deviates from a regular α-helix. However, due to the presence of $d_{\alpha N(i,i+3)}$ NOEs in combination with strong $d_{NN(i,i+1)}$ NOEs and small $^3J_{H^N H^\alpha}$ coupling constants for the residues Glu^{105} and Asn^{106}, this helix is determined to start at Glu^{105}.

In Fig. 1B the consensus binding-site residues of *Anacystis nidulans* flavodoxin are underlined (Stockman et al., 1990). The corresponding residues in *A. chroococcum* flavodoxin also are located near the FMN molecule, since all of them are affected in the one-electron-reduced flavodoxin (Fig. 5). As for other flavodoxins (Van Mierlo et al., 1990b; Clubb et al., 1991; Stockman et al., 1993; Peelen and Vervoort, 1994), the loop-containing residues Ser^{10}–Thr^{16} must be involved in the binding of the FMN phosphate, because low-field amide-proton chemical shift values, caused by hydrogen bonding to the negatively charged phosphate group, are observed for Ser^{10} (8.49 ppm), Asn^{11} (10.84 ppm), Thr^{12} (9.89 ppm), Lys^{14} (11.15 ppm) and Thr^{15} (10.72 ppm) (see Supplementary Material, Table S2). A $d_{NN(i,i+2)}$ NOE connectivity between the amide protons of Asn^{11} and Gly^{13} indicates the presence of a reverse turn (Wüthrich, 1986) between strand β1 and helix α1. This sheet–turn–helix motif has in all flavodoxin structures been identified as the FMN-phosphate binding region (Watenpaugh et al., 1973; Burnett et al., 1974; Ludwig et al., 1976; Smith et al., 1977,1983; Fukuyama et al., 1990; Van Mierlo et al., 1990a; Stockman et al., 1990; Watt et al., 1991). The residues in the regions of *A. chroococcum* flavodoxin corresponding to the consensus FMN binding-site residues Pro^{55}–Glu^{61} and Ala^{88}–Gln^{99} of the flavodoxin from *A. nidulans*, are located close to the FMN NH(3). This can be concluded from the fact that NOE connectivities between Thr^{57}, Tyr^{103}, Asn^{106}, Phe^{107}, Leu^{108}, Asp^{109} and the FMN NH(3) proton are observed, which are shown in Fig. 9.

Zhou and Swenson (1995) reported that for the flavodoxin from *Desulfovibrio vulgaris* negatively charged amino acid residues located near the FMN contribute to the low midpoint potential of the semiquinone–hydroquinone couple (–440 mV; Curley et al., 1991). The midpoint potential of the semiquinone–hydroquinone couple of *A. chroococcum* flavodoxin is more negative by 82 mV, i.e. –522 mV (Deistung and Thorneley, 1986). Zhou and Swenson (1995) observed an average increase in the midpoint potential of 15 mV when a negatively charged residue was mutated to a neutral residue. If this is extended to *A. chroococcum* flavodoxin, this means that this flavodoxin should have about five more negatively charged residues surrounding the FMN than the flavodoxin from *D. vulgaris*. From the residues in *A. chroococcum* flavodoxin affected by the one-electron-reduced FMN, 13 are negatively charged (Fig. 5). From the corresponding residues, as deduced by the alignment in Fig. 1B, in *D. vulgaris* flavodoxin only eight residues are negatively charged. Although this is exactly five negatively charged residues less, one should bear in mind that this way of comparison can only be an estimate and that eventually the 3D structures should be compared. Yet, it can savely be concluded that indeed more negatively charged amino acids surround the FMN in *A. chroococcum* flavodoxin.

When compared to *D. vulgaris* flavodoxin, it is interesting to note that the additional negatively charged residues in *A. chroococcum* flavodoxin are mainly located in the extra loops Gly^{61}–Glu^{71} and Trp^{129}–Val^{148}. Mutations of the negatively charged residues in these loops need to be performed in order to test the hypothesis whether or not these extra loop residues in the flavodoxin from *A. chroococcum* are responsible for its low redox potential. A characteristic feature of the flavodoxins is the asymmetric distribution of the charged amino acid residues; the negatively charged residues are clustered around the FMN binding site, whereas no positively charged residues are observed in the vicinity of the isoalloxazine ring (Watenpaugh et al., 1973; Burnett et al., 1974; Smith et al., 1983). For the flavodoxin of *A. chroococcum*, 13 of the 29 acidic residues are located in the regions affected by the one-electron-reduced FMN, whereas only one basic residue is located in these regions (Fig. 5). Positively charged residues are mainly located in helix α1 (Fig. 5). Whether or not this is important for the stabilisation of the negatively charged FMN phosphate group, possibly in combination with the dipole moment of helix α1 (Hol et al., 1978), has to be further investigated. As no positively charged helix α1 is observed in the flavodoxins from *D. vulgaris* and *A. nidulans* (Fig. 1B) (Watt et al., 1991; Stockman et al., 1993), the former seems not to be the case. On the other hand, this positively charged helix, in combination with the negatively charged cluster around FMN, may play an important role in the formation of the electron-transfer complex, and thus for electron transfer, with the Fe protein of the nitrogenase enzyme system. For the electron transfer between flavodoxins and cytochrome *c*, electrostatic interactions were proven to be important (Simondson et al., 1982; Weber and Tollin, 1985).

Indeed, electrostatic interactions are important for the complex formation between the flavodoxin and Fe protein

from *A. chroococcum*, since an increase in ionic strength leads to a weaker complex as the intensities of the uncomplexed flavodoxin amide resonances increase upon addition of KCl (Fig. 7). Furthermore, the ^{15}N chemical shifts of the flavodoxin amino acid residues involved in complex formation, return towards their uncomplexed chemical shift values (Figs. 7 and 8). Only a few flavodoxin chemical shift changes are observed upon titration of the flavodoxin with Fe protein, and although they are small, they are significant. Larger effects would be expected if the Fe protein were to have been in excess. However, for practical reasons this experiment could not be performed. It is interesting to note that the observed chemical shift changes are all located within the same part of the molecule, namely in the region of the extra short loop Gly^{61}–Glu^{71}. This loop is located near the FMN binding site, since the amide resonances of the residues in this loop are affected by the one-electron-reduced FMN (Fig. 5). Furthermore, this loop must be located at the surface of the protein, as most of the amide protons in this loop exchange within 2 h after redissolving the protein in D_2O. The ^{15}N chemical shifts of the amide of Ser^{68} and the amino side chains of Asn^{11} and Asn^{72} significantly change when flavodoxin is titrated with the Fe protein. Residues Ser^{68} and Asn^{72} are both located in the above-mentioned extra loop, whereas Asn^{11} is not. However, a clear NOE connectivity is observed between the amide proton of the extra loop residue Glu^{71} and one of the amino side-chain protons of Asn^{11}. The observation that the loop residues Ser^{68} and Asn^{72} and the nearby Asn^{11} are influenced upon complexation of flavodoxin with the Fe protein indicates that this loop, which is missing in the shorter-chain flavodoxins, must play an important role in complex formation between flavodoxin and the nitrogenase enzyme system. For these residues only the ^{15}N, and not the ^{1}H chemical shifts change significantly when the Fe protein is titrated. This suggests that the interaction of these residues with the Fe protein is not via the amide and side-chain amino protons, but via the oxygen atoms of the backbone carbonyl of Ser^{67} and the side-chain carbonyls of Asn^{11} and Asn^{72}. This hypothesis is reasonable, since interactions of acidic atoms are expected to be important for complexation with the Fe protein, as the FMN is surrounded by acidic residues. For this reason, the acidic residues Glu^{62}, Asp^{69} and Glu^{71} in this extra loop may play an important role in complex formation. However, due to the nature of a 2D ^{1}H-^{15}N HSQC experiment the side-chain atoms of these residues cannot be observed.

The flavodoxin from *K. pneumoniae* forms a stronger complex with its Fe protein when MgADP is present (Thorneley and Deistung, 1988). The addition of MgADP shows an additional ^{15}N chemical shift change for the three residues in *A. chroococcum* flavodoxin involved in complex formation with the Fe protein (Fig. 8), indicating a change in the nature of this complex, possibly due to a stronger interaction. Especially the side-chain amino group of Asn^{11} is influenced by the addition of MgADP (Fig. 8). The binding of MgATP and MgADP to the Fe protein results in a change in conformation of the Fe protein, which is accompanied by a decrease in the redox potential of the 4Fe4S cluster of the Fe protein. The 2.9-Å resolution X-ray crystal structure of the Fe protein from *A. vinelandii* shows a nucleotide binding site to be located at the subunit interface of the dimeric molecule (Georgiadis et al., 1992). The change in stability of the flavodoxin–Fe-protein complex we observe most likely arises from a change in conformation of the Fe protein, resulting from MgADP binding at this site. Further studies have to be performed to elucidate the exact role of MgADP.

From this titration study it is concluded that the short extra loop Gly^{61}–Glu^{71} in the flavodoxin from *A. chroococcum* is of importance for the complexation with the Fe protein of the nitrogenase enzyme complex, and that therefore this loop may play an important role in the electron transfer to nitrogenase.

From the secondary solution structure information obtained in this study it can be concluded that the structure of the flavodoxin from *A. chroococcum* very much will resemble those of other flavodoxins. This structural information, therefore, does not provide insight as to what causes the very low semiquinone–hydroquinone midpoint potential for this particular flavodoxin. However, the presence of additional negatively charged residues surrounding the FMN is discussed to cause this low midpoint potential.

Acknowledgements

This study was supported by the Dutch Foundation for Chemical Research (SON) with financial aid from the Netherlands Organisation for Scientific Research (NWO) and the EU-FLAPS network (HCM contract CHRX-CT93-0166). Collaboration between Robert Eady and Robert Robson in sequencing *nifF* was facilitated by NATO Grant 04-0058-88. We thank Neville Henderson for skilled microbiological technical support and Geerten Vuister and Ad Bax for providing us some of the original pulse programs. Furthermore, we want to thank Carlo van Mierlo and Elles Steensma for our fruitful discussions and Prof. Cees Veeger for critically reading the manuscript. The 600 MHz NMR experiments were performed at the SON/NWO National HF-NMR Facility at Nijmegen, The Netherlands.

References

Bagby, S., Barker, P.D., Hill, H.A.O., Sanghera, G.S., Dunbar, B., Ashby, G.A., Eady, R.R. and Thorneley, R.N.F. (1991) *Biochem. J.*, **277**, 313–319.

Bartels, C., Xia, T., Billeter, M., Güntert, P. and Wüthrich, K. (1995) *J. Biomol. NMR*, **5**, 1–10.

Bax, A. and Davis, D.G. (1985) *J. Magn. Reson.*, **65**, 355–360.

Bennet, L.T., Jacobson, M.R. and Dean, D.R. (1988) *J. Biol. Chem.*, **263**, 1364–1369.

Bloembergen, N. (1957) *J. Chem. Phys.*, **27**, 572–573.

Bodenhausen, G. and Ruben, D.J. (1980) *Chem. Phys. Lett.*, **69**, 185–189.

Burnett, R.M., Darling, G.D., Kendall, D.S., LeQuesne, M.E., Mayhew, S.G., Smith, W.W. and Ludwig, M.L. (1974) *J. Biol. Chem.*, **249**, 4383–4392.

Cavanagh, J., Palmer III, A.G., Wright, P.E. and Rance, M. (1991) *J. Magn. Reson.*, **91**, 429–436.

Cavanagh, J. and Rance, M. (1990) *J. Magn. Reson.*, **88**, 72–85.

Clubb, R.T., Thanabal, V., Osborne, C. and Wagner, G. (1991) *Biochemistry*, **30**, 7718–7730.

Curley, G.P., Carr, M.C., Mayhew, S.G. and Voordouw, G. (1991) *Eur. J. Biochem.*, **202**, 1091–1100.

Deistung, J. and Thorneley, R.N.F. (1986) *Biochem. J.*, **239**, 69–75.

Dente, L., Cesareni, G. and Corteses, R. (1983) *Nucleic Acids Res.*, **11**, 1645–1655.

Deveraux, J., Haeberli, P. and Smithies, O. (1985) *Nucleic Acids Res.*, **12**, 387–395.

Eady, R.R., Richardson, T.H., Miller, R.W., Hawkins, M. and Lowe, D.J. (1988) *Biochem. J.*, **256**, 189–196.

Evans, D.J., Jones, R., Woodley, P.R., Wilborn, J.R. and Robson, R.L. (1991) *J. Bacteriol.*, **173**, 5457–5469.

Frenkiel, T., Bauer, C., Carr, M.D., Birdsall, B. and Feeney, J. (1990) *J. Magn. Reson.*, **90**, 420–425.

Fritz, J., Müller, F. and Mayhew, S.G. (1973) *Helv. Chim. Acta*, **56**, 2250–2254.

Fukuyama, K., Wakabayashi, S., Matsubara, H. and Rogers, L.J. (1990) *J. Biol. Chem.*, **265**, 15804–15812.

Georgiadis, M.M., Komiya, H., Chakrabarti, P., Woo, D., Kornuc, J.J. and Rees, D.C. (1992) *Science*, **257**, 1653–1659.

Griesinger, C., Otting, G., Wüthrich, K. and Ernst, R.R. (1988) *J. Am. Chem. Soc.*, **110**, 7870–7872.

Grzesiek, S. and Bax, A. (1992a) *J. Magn. Reson.*, **99**, 201–207.

Grzesiek, S. and Bax, A. (1992b) *J. Am. Chem. Soc.*, **114**, 6291–6293.

Grzesiek, S. and Bax, A. (1992c) *J. Magn. Reson.*, **96**, 432–440.

Grzesiek, S. and Bax, A. (1993) *J. Biomol. NMR*, **3**, 185–204.

Güntert, P. and Wüthrich, K. (1992) *J. Magn. Reson.*, **96**, 403–407.

Hol, W.G.J., Van Duijnen, P.T. and Berendsen, H.J.C. (1978) *Nature*, **273**, 443–446.

Ikura, M., Bax, A., Clore, G.M. and Gronenborn, A.M. (1990) *J. Am. Chem. Soc.*, **112**, 9020–9022.

Jahnke, W. and Kessler, H. (1994) *J. Biomol. NMR*, **4**, 735–740.

Jones, R., Woodley, P. and Robson, R.L. (1984) *Mol. Gen. Genet.*, **197**, 318–327.

Kay, L.E., Keifer, P. and Saarinen, T. (1992) *J. Am. Chem. Soc.*, **114**, 10663–10665.

Kim, J. and Rees, C.R. (1994) *Biochemistry*, **33**, 389–397.

Kontaxis, G., Stonehouse, J., Laue, E.D. and Keeler, J. (1994) *J. Magn. Reson. Ser. A*, **111**, 70–76.

Ludwig, M.L., Burnett, R.M., Darling, G.D., Jordan, S.R., Kendall, D.S. and Smith, W.W. (1976) In *Flavins and Flavoproteins* (Ed. Singer, T.P.), Elsevier, Amsterdam, The Netherlands, pp. 393–404.

Marion, D., Driscoll, P.C., Kay, L.E., Wingfield, P.T., Bax, A., Gronenborn, A.M. and Clore, G.M. (1989a) *Biochemistry*, **28**, 6150–6156.

Marion, D., Ikura, M. and Bax, A. (1989b) *J. Magn. Reson.*, **84**, 425–430.

Marion, D., Ikura, M., Tschudin, R. and Bax, A. (1989c) *J. Magn. Reson.*, **85**, 393–399.

Marion, D. and Wüthrich, K. (1983) *Biochem. Biophys. Res. Commun.*, **113**, 967–724.

Mayhew, S.G. and Tollin, G. (1992) In *Chemistry and Biochemistry of Flavoenzymes* (Ed. Müller, F.), CRC Press, Boca Raton, FL, pp. 389–426.

Orengo, C.A., Jones, D.T. and Thornton, J.M. (1994) *Nature*, **372**, 631–634.

Palmer III, A.G., Cavanagh, J., Wright, P.E. and Rance, M. (1991) *J. Magn. Reson.*, **93**, 151–170.

Peelen, S. and Vervoort, J. (1994) *Arch. Biochem. Biophys.*, **314**, 291–300.

Sanger, F., Nicklen, S. and Coulsen, A.R. (1977) *Proc. Natl. Acad. Sci. USA*, **82**, 1074–1078.

Simondson, R.P., Weber, P.C., Salemne, F.R. and Tollin, G. (1982) *Biochemistry*, **21**, 6366–6375.

Smith, W.W., Burnett, R.M., Darling, G.D. and Ludwig, M.L. (1977) *J. Mol. Biol.*, **117**, 195–225.

Smith, W.W., Pattridge, K.A., Ludwig, M.L., Petsko, G.A., Tsernoglou, D., Tanaka, M. and Yasanobu, K.T. (1983) *J. Mol. Biol.*, **165**, 737–755.

Solomon, I. (1955) *Phys. Rev.*, **99**, 559–565.

Stockman, B.J., Euvrard, A., Kloosterman, D.A., Scahill, T.A. and Swenson, R.P. (1993) *J. Biomol. NMR*, **3**, 133–149.

Stockman, B.J., Krezel, A.M., Markley, J.L., Leonhardt, K.G. and Strauss, N.A. (1990) *Biochemistry*, **29**, 9600–9609.

Stonehouse, J., Shaw, G.L., Keeler, J. and Laue, E.D. (1994) *J. Magn. Reson. Ser. A*, **107**, 178–184.

Thorneley, R.N.F. and Deistung, J. (1988) *Biochem. J.*, **253**, 587–595.

Van Mierlo, C.P.M., Müller, F. and Vervoort, J. (1990a) *Eur. J. Biochem.*, **189**, 589–600.

Van Mierlo, C.P.M., Van der Sanden, B.P.J., Van Woensel, P., Müller, F. and Vervoort, J. (1990b) *Eur. J. Biochem.*, **194**, 199–216.

Vuister, G.W. and Bax, A. (1993) *J. Am. Chem. Soc.*, **115**, 7772–7777.

Vuister, G.W., Kim, S.-J., Wu, C. and Bax, A. (1994) *Biochemistry*, **33**, 10–16.

Watenpaugh, K.D., Sieker, L.C. and Jensen, L. (1973) *Proc. Natl. Acad. Sci. USA*, **70**, 3857–3860.

Watt, W., Tulinsky, A., Swenson, R.P. and Watenpaugh, K.D. (1991) *J. Mol. Biol.*, **218**, 195–208.

Weber, P.C. and Tollin, G. (1985) *J. Biol. Chem.*, **260**, 5568–5573.

Wishart, D.S., Sykes, B.D. and Richards, F.M. (1992) *Biochemistry*, **31**, 1647–1651.

Wishart, D.S. and Sykes, B.D. (1994) *J. Biomol. NMR*, **4**, 171–180.

Wishart, D.S., Bigam, C.G., Yao, J., Abildgaard, F., Dyson, H.J., Oldfield, E., Markley, J.L. and Sykes, B.D. (1995) *J. Biomol. NMR*, **6**, 135–140.

Wüthrich, K. (1986) *NMR of Proteins and Nucleic Acids*, Wiley, New York, NY.

Yates, M.G. (1972) *Febs Lett.*, **27**, 63–67.

Zhou, Z. and Swenson, R.P. (1995) *Biochemistry*, **34**, 3183–3192.

Zuiderweg, E.R.P. and Fesik, S.W. (1989) *Biochemistry*, **28**, 2387–2391.